Electronic Supplementary Information (ESI)

The correspondence between conformational and chromophoric properties of amorphous conjugated polymer in mesoscale condensed system

Chun I Wang, Chih H. Hsu, and Chi C. Hua*

Department of Chemical Engineering, National Chung Cheng University, Chia-Yi 62102, Taiwan, R.O.C.

S1. Descriptions and Validation of the Force Field

Fig. S1 presents two different torsion angles of the MEH-PPV backbone, for which the corresponding torsional potentials need further modifications. Following the previous report of Friesner's group,[1] the modifications are performed by varying the C_i parameters within the standard functional form in the OPLS force field:

$$U(\phi) = \frac{1}{2}\left[C_1\left(1+cos(\phi)\right) + C_2\left(1-cos(2\phi)\right) + C_3\left(1+cos(3\phi)\right) - C_4\left(1-cos(4\phi)\right)\right] \qquad (1)$$

In this equation, ϕ denotes the torsion angle, and C_1, C_2, C_3, C_4 are adjustable parameters whose values are listed in Table S1.

The partial atomic charges presently adopted for MEH-PPV and C_{60} molecules are listed in Table S2-S3. Given that partial atomic charges on the C_{60} molecule are generally small (<<

0.1), their effects were often neglected in the AMD simulation. However, partial atomic changes may play an important role in the QC calculation when the effect of electrostatic environment is taken into account. In this work, therefore, partial atomic charges of C_{60} are incorporated in all AMD simulations.

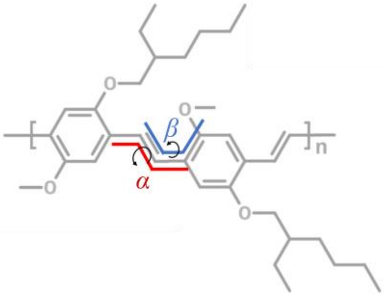

Fig. S1. Cartoons showing two different torsion angles of the MEH-PPV backbone. The torsions of interest, α and β, are marked by the arrows, and the atoms defining them are highlighted by the red and blue bars, respectively.

Table S1. Modified parameter values for the OPLS torsional potentials of MEH-PPV.

Unit: *k*cal/mol	Torsion angle α	Torsion angle β
C_1	0.000	0.316
C_2	10.200	3.000
C_3	0.000	-0.947
C_4	-1.200	-0.200

Using the OPLS-based force field, we obtain a density of 1.02 g/cm^3 at the end of the annealing procedure for pure MEH-PPV system, a result in close agreement with the experimental value of 0.98 g/cm^3.[2] The excitation energies of MEH-PPV for several low-lying excited states, as have been estimated using the chain conformation generated by the present

AMD simulation, are also in fair agreement with prior experimental and theoretical results (see Table S4).

Table S2. List of the computed partial atomic charges on a MEH-PPV monomer (in the plot below, grey beads, red beads, and white beads refer to carbon, oxygen, and hydrogen atoms, respectively).

Atom Index	Charge	Atom Index	Charge	Atom Index	Charge
1	-0.061577271	16	0.007068729	31	-0.077015938
2	0.248974062	17	0.008348395	32	0.013665395
3	-0.290170938	18	0.110191062	33	0.013870062
4	0.074269395	19	0.151132395	34	0.008007395
5	0.153431062	20	0.074704729	35	-0.054155938
6	-0.196168605	21	0.095288395	36	0.000384729
7	-0.118250605	22	0.028327062	37	0.010291062
8	-0.152148938	23	-0.017299271	38	0.016148729
9	-0.264239271	24	0.167251729	39	-0.009787605
10	-0.285766605	25	-0.039355271	40	0.020050729
11	0.140392395	26	-0.046583605	41	0.148118729
12	0.042786395	27	-0.102866605	42	-0.032211605
13	0.010816729	28	0.017062062	43	-0.031080605
14	0.007722729	29	0.022440729	Tail	0.000000010
15	0.180138729	30	0.007795062	Head	0.000000010

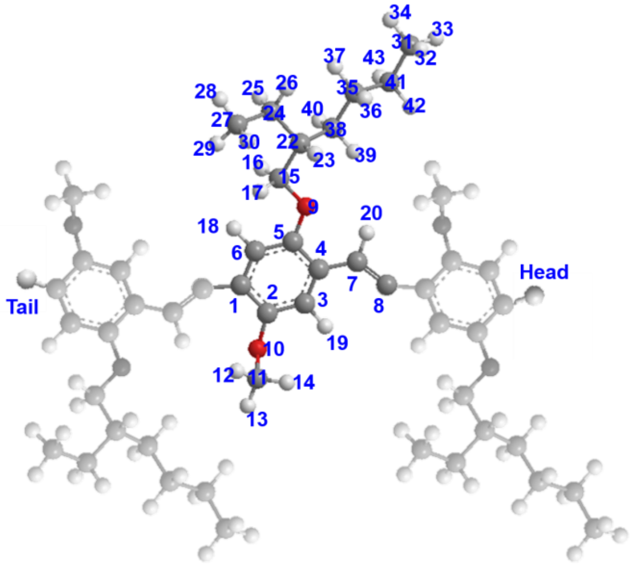

Table S3. List of the computed partial atomic charges on a C_{60} molecule and the associated geometrical coordinates of each carbon atom.

Atom Index	X [Å]	Y [Å]	Z [Å]	Charge
1	1.56	4.90	5.61	0.014412
2	2.20	3.96	6.52	-0.018974
3	3.56	3.70	6.39	0.013996
4	4.35	4.32	5.35	-0.004232
5	3.71	5.13	4.45	0.007569
6	2.31	5.45	4.57	-0.013758
7	1.22	2.90	6.93	0.007150
8	3.99	2.33	6.72	-0.010862
9	5.28	3.31	4.94	0.007528
10	3.99	5.02	3.01	0.003799
11	1.73	5.52	3.24	-0.016335
12	0.28	4.28	5.37	-0.000125
13	4.91	4.04	2.59	-0.014838
14	5.57	3.16	3.57	0.004197
15	4.60	3.22	1.43	-0.005826
16	5.70	1.82	2.98	-0.000567
17	1.67	1.58	7.14	0.008085
18	5.05	2.10	5.74	0.003866
19	5.10	1.84	1.65	-0.010023
20	5.13	0.83	5.16	-0.005253
21	3.07	1.32	7.01	0.012270
22	2.76	5.15	2.26	0.003115
23	0.48	4.92	2.99	-0.008430
24	0.94	0.47	6.59	0.007199
25	-0.29	4.38	4.10	-0.010925
26	-0.01	3.15	6.19	0.002248
27	0.14	4.16	1.76	-0.006096
28	-1.11	3.28	3.57	0.006208
29	-0.72	2.05	5.67	0.012634
30	5.46	0.67	3.77	0.007218
31	2.47	4.44	1.07	-0.010094
32	3.20	-0.02	6.41	0.003952
33	-0.83	3.15	2.12	0.007999
34	-1.29	2.11	4.31	-0.013671
35	-0.24	0.68	5.90	-0.018908
36	-0.54	-0.08	4.67	0.007510
37	1.88	-0.54	6.14	-0.010892
38	4.26	-0.27	5.54	-0.005224

To be continued in the next page

Atom Index	X [Å]	Y [Å]	Z [Å]	Charge
39	3.96	-1.00	4.32	0.012255
40	-1.18	0.80	3.72	0.003138
41	-0.84	0.70	2.38	0.007143
42	0.06	-0.37	1.87	-0.010882
43	-0.70	1.89	1.54	0.002210
44	3.48	3.47	0.65	-0.000523
45	2.67	-1.50	4.06	-0.005806
46	1.12	3.93	0.79	0.007499
47	1.30	2.62	0.21	-0.004155
48	1.60	-1.29	4.98	0.013930
49	4.77	-0.50	3.24	0.003814
50	4.26	-0.42	1.93	0.011940
51	0.36	-1.08	4.23	-0.016330
52	0.69	-1.21	2.80	0.012662
53	0.39	1.60	0.62	-0.000174
54	0.88	0.25	0.84	-0.014806
55	2.12	-1.36	2.71	0.004172
56	2.74	2.34	0.11	0.006218
57	4.36	0.77	1.16	-0.006087
58	2.92	-0.94	1.64	-0.008406
59	3.19	1.03	0.34	0.011937
60	2.23	-0.02	0.75	0.014329

Table S4. List of excitation energies (in unit of eV) for several low-lying excited states for pure MEH-PPV and MEH-PPV/C_{60} hybrid systems.

	Pure MEH-PPV	MEH-PPV/C_{60}	7-mer PPV[3]	14-mer PPV[4]	MEH-PPV thin film[5]
S_1	2.76 ± 0.10	2.75 ± 0.11	3.03	2.65	2.44
S_2	2.91 ± 0.09	2.89 ± 0.09	3.34	-	-
S_3	3.03 ± 0.07	3.01 ± 0.08	3.70	-	-
S_4	3.16 ± 0.07	3.15 ± 0.08	4.05	-	-
S_5	3.27 ± 0.06	3.27 ± 0.068	-	-	-

S2. Evaluation Scheme of the Correlation between Two Distribution Functions

According to the discussion in the main text, we denote the population distribution of chain conformation as X, and that of the chromophore as Y, both being functions of the conformational factor, i.e., X (f_{orient}) and Y (f_{orient}). To evaluate the correlation between the two, the so-called sample correlation coefficient, r, is defined as[6]

$$r = \frac{1}{n-1}\sum_{i=1}^{n}\left[\frac{X_i(f_i)-\bar{X}}{S_X(f_i)}\right]\left[\frac{Y_i(f_i)-\bar{Y}}{S_Y(f_i)}\right] \tag{2}$$

In the equation above, n is the total number of variables used for f_{orient} (or f_{planar}), $\bar{X}$ and $\bar{Y}$ denote the mean values, and S_X and S_Y represent the standard variances defined as

$$S_X^2 = \sum_{i=1}^{n}(X(f_i)-\bar{X})^2/(n-1) \tag{3}$$

$$S_Y^2 = \sum_{i=1}^{n}(Y(f_i)-\bar{Y})^2/(n-1) \tag{4}$$

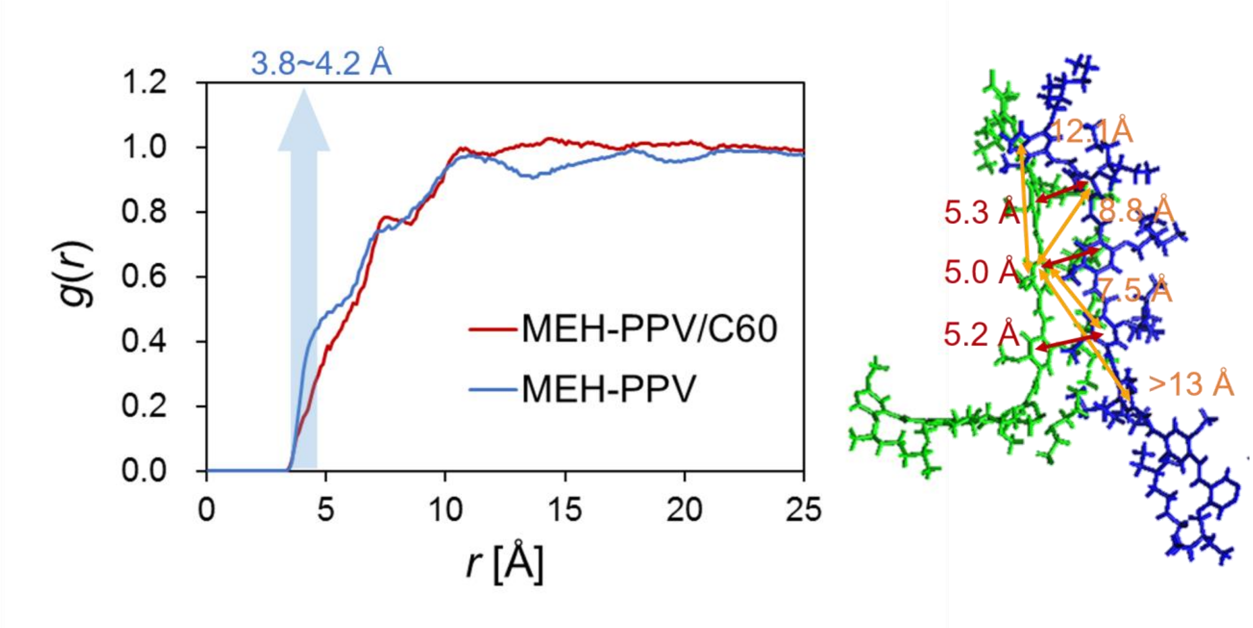

Fig. S2. Radial distribution functions (RDFs) of the phenyl-ring pair at different MEH-PPV chains for pure MEH-PPV and MEH-PPV/C_{60} hybrid systems. The RDF at short distances (i.e., *r* = 3~15 Å) reveals the existence of complicated structural features (see illustrations in the snapshot), and the formation of compact π-π staking (at *r* = 3.8~4.2 Å) can be seen to be rare in both systems.

Pure MEH-PPV

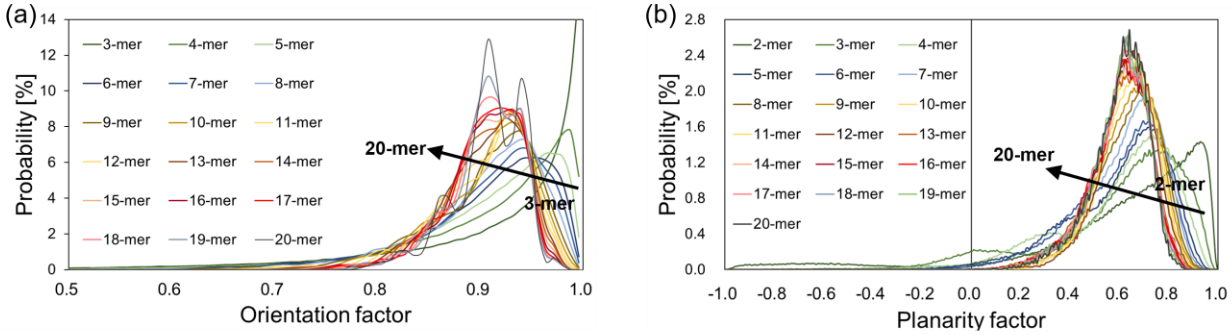

MEH-PPV/C_{60} Hybrid

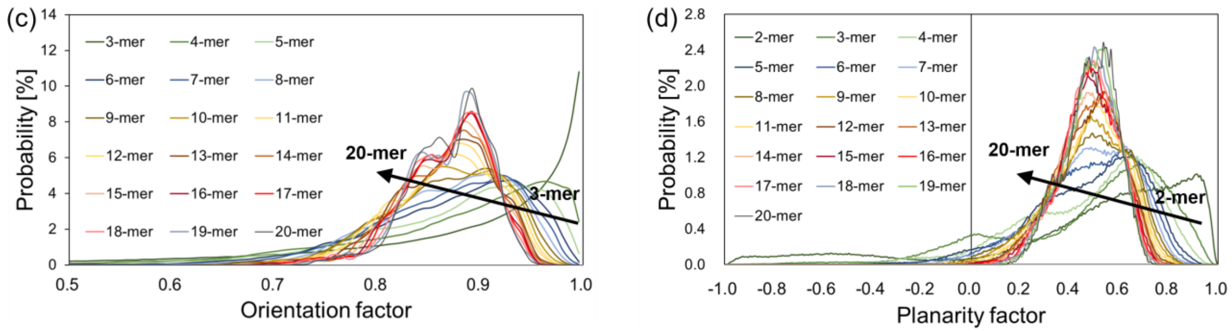

Fig. S3. Population distributions of the AMD-characterized conformational units based on various choices of the segmental length (i.e., 2~20-mer): (a, c) orientation factor and (b, d) planarity factor for pure MEH-PPV (top) and MEH-PPV/C_{60} hybrid (bottom) systems.

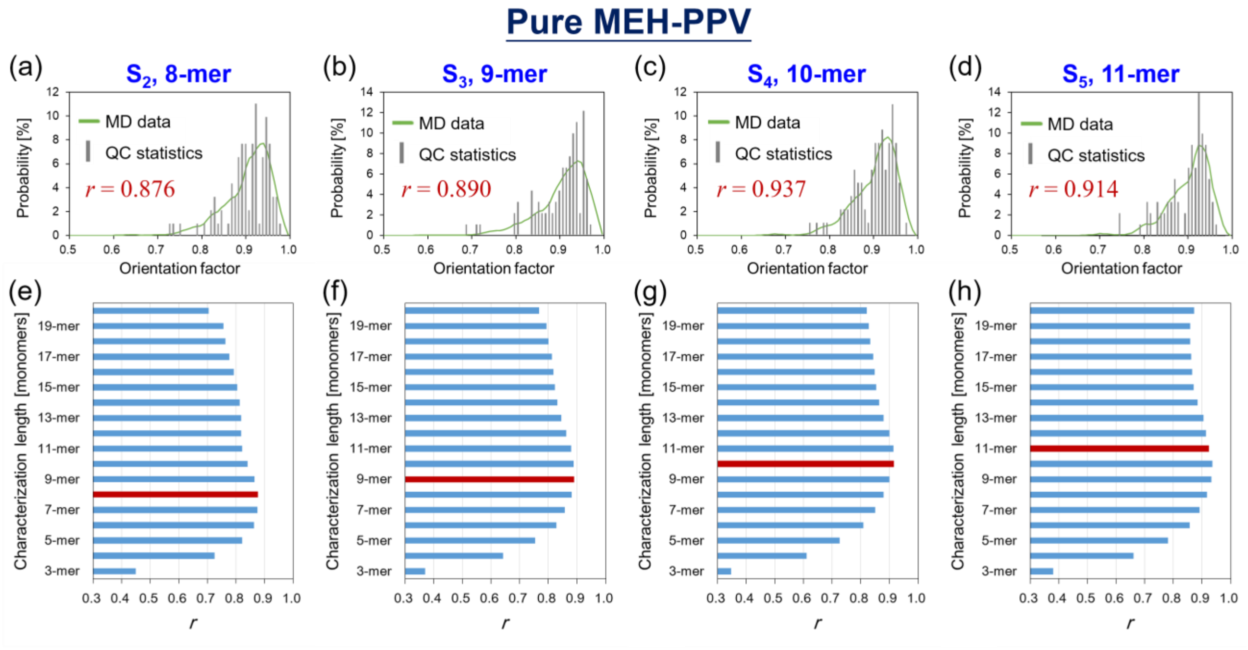

Fig. S4. Population histograms of the chromophore identified in the QC calculation as a function of the orientation factor, as compared with the population distributions (green line) of the AMD-characterized conformational unit for pure MEH-PPV system: (a) 8-mer for the S_2 state, (b) 9-mer for the S_3 state, (c) 10-mer for the S_4 state, and (d) 11-mer for the S_5 state, where the number of monomers utilized in each case reflects the average conjugation length for a particular excited state; (e-h) the correlation coefficient, *r*, as a function of the segmental length used in the evaluation of the orientation factor, where the red bars correspond to the correlation coefficients indicated in (a-d).

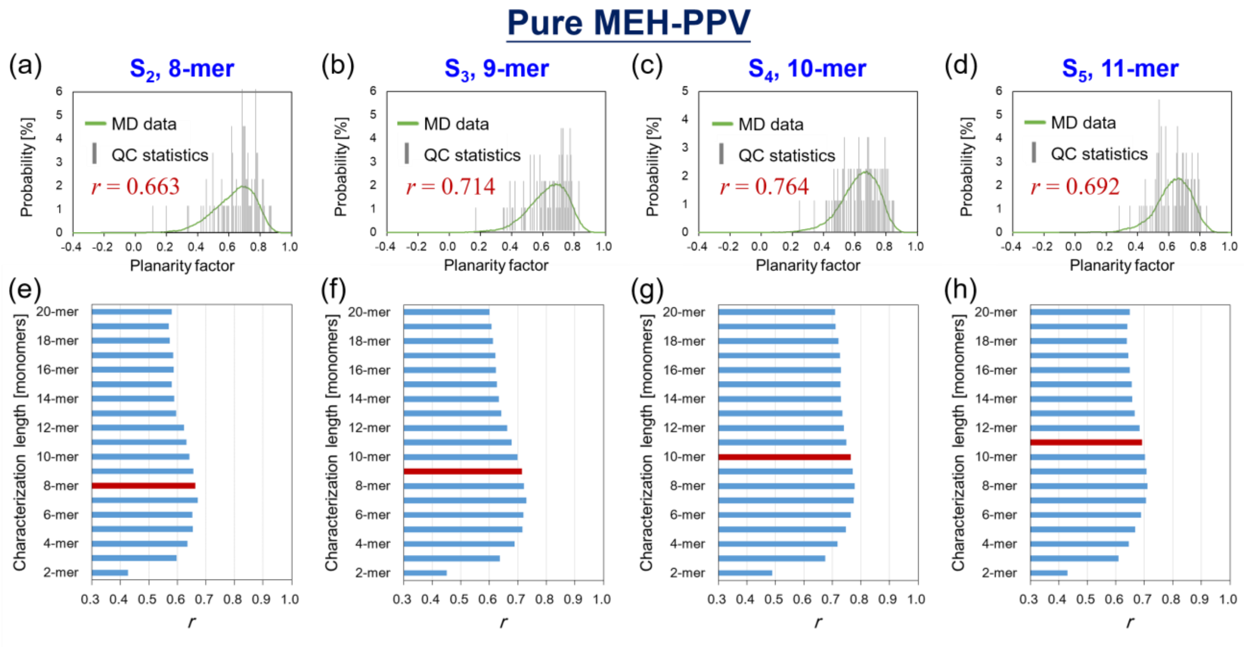

Fig. S5. Population histograms of the chromophore identified in the QC calculation as a function of the planarity factor, as compared with the population distributions (green line) of the AMD-characterized conformational unit for pure MEH-PPV system: (a) 8-mer for the S_2 state, (b) 9-mer for the S_3 state, (c) 10-mer for the S_4 state, and (d) 11-mer for the S_5 state; (e-h) the correlation coefficient, *r*, as a function of the segmental length used in the evaluation of the planarity factor, where the red bars correspond to the correlation coefficients indicated in (a-d).

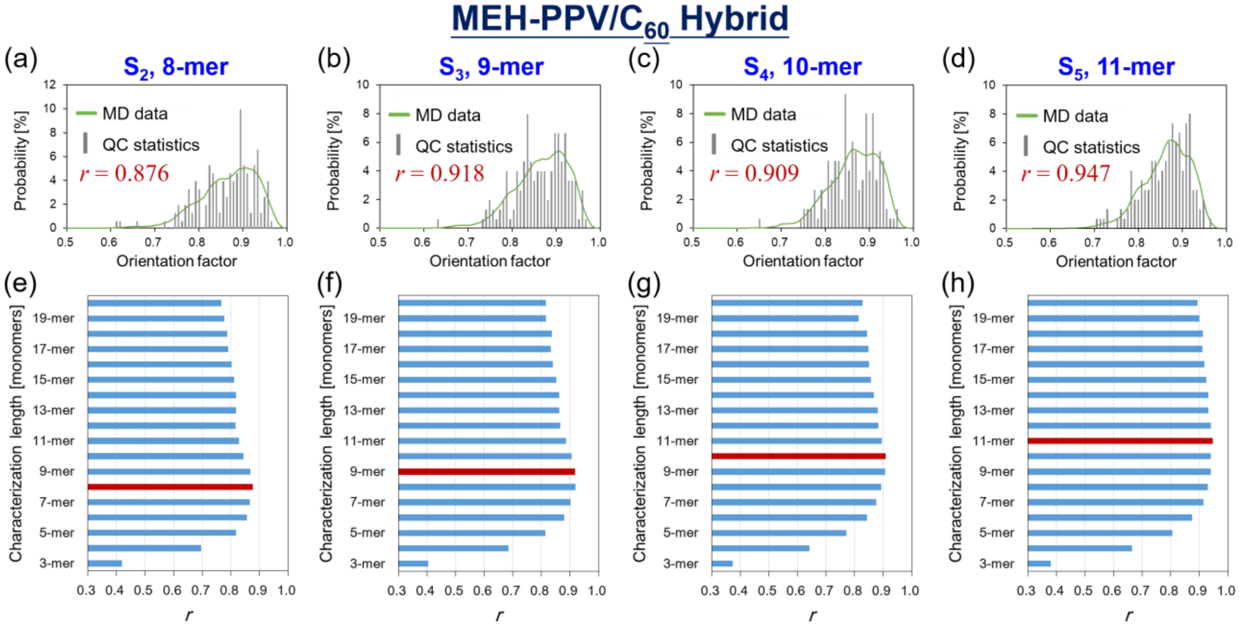

Fig. S6. Population histograms of the chromophore identified in the QC calculation as a function of the orientation factor, as compared with the population distributions (green line) of the AMD-characterized conformational unit for MEH-PPV/C_{60} hybrid system: (a) 8-mer for the S_2 state, (b) 9-mer for the S_3 state, (c) 10-mer for the S_4 state, and (d) 11-mer for the S_5 state; (e-h) the correlation coefficient, *r*, as a function of the segmental length used in the evaluation of the orientation factor, where the red bars correspond to the correlation coefficients indicated in (a-d).

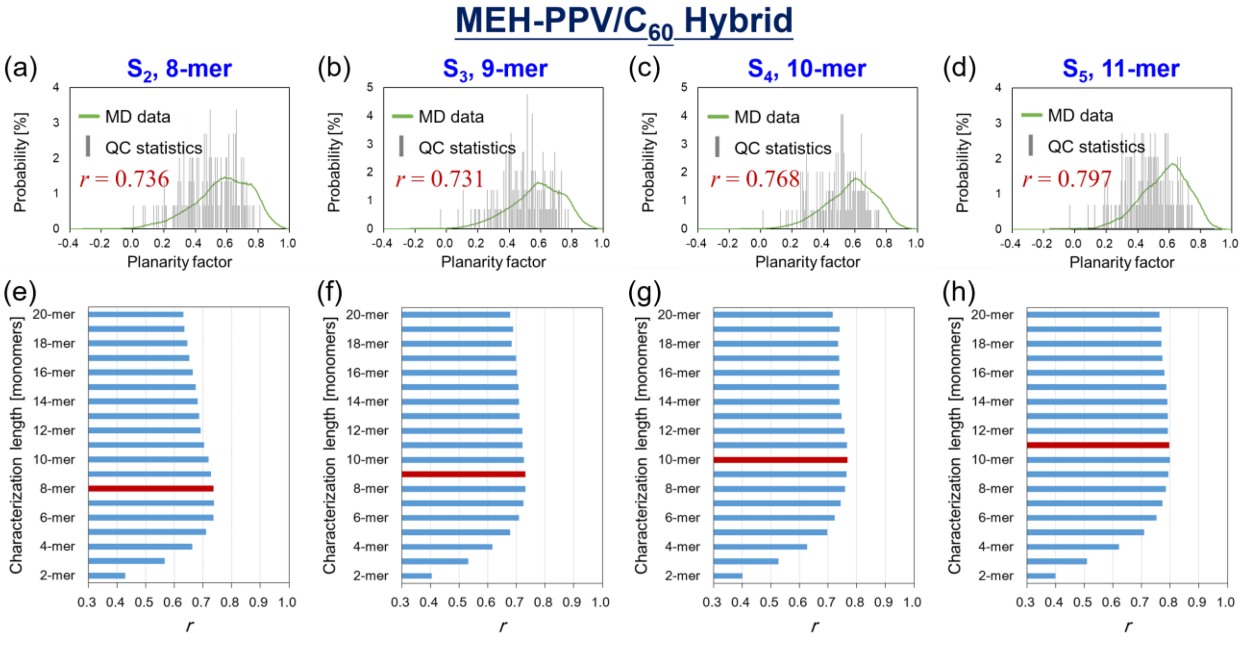

Fig. S7. Population histograms of the chromophore identified in the QC calculation as a function of the planarity factor, as compared with the population distributions (green line) of the AMD-characterized conformational unit for MEH-PPV/C_{60} hybrid system: (a) 8-mer for the S_2 state, (b) 9-mer for the S_3 state, (c) 10-mer for the S_4 state, and (d) 11-mer for the S_5 state; (e-h) the correlation coefficient, *r*, as a function of the segmental length used in the evaluation of the planarity factor, where the red bars correspond to the correlation coefficients indicated in (a-d).

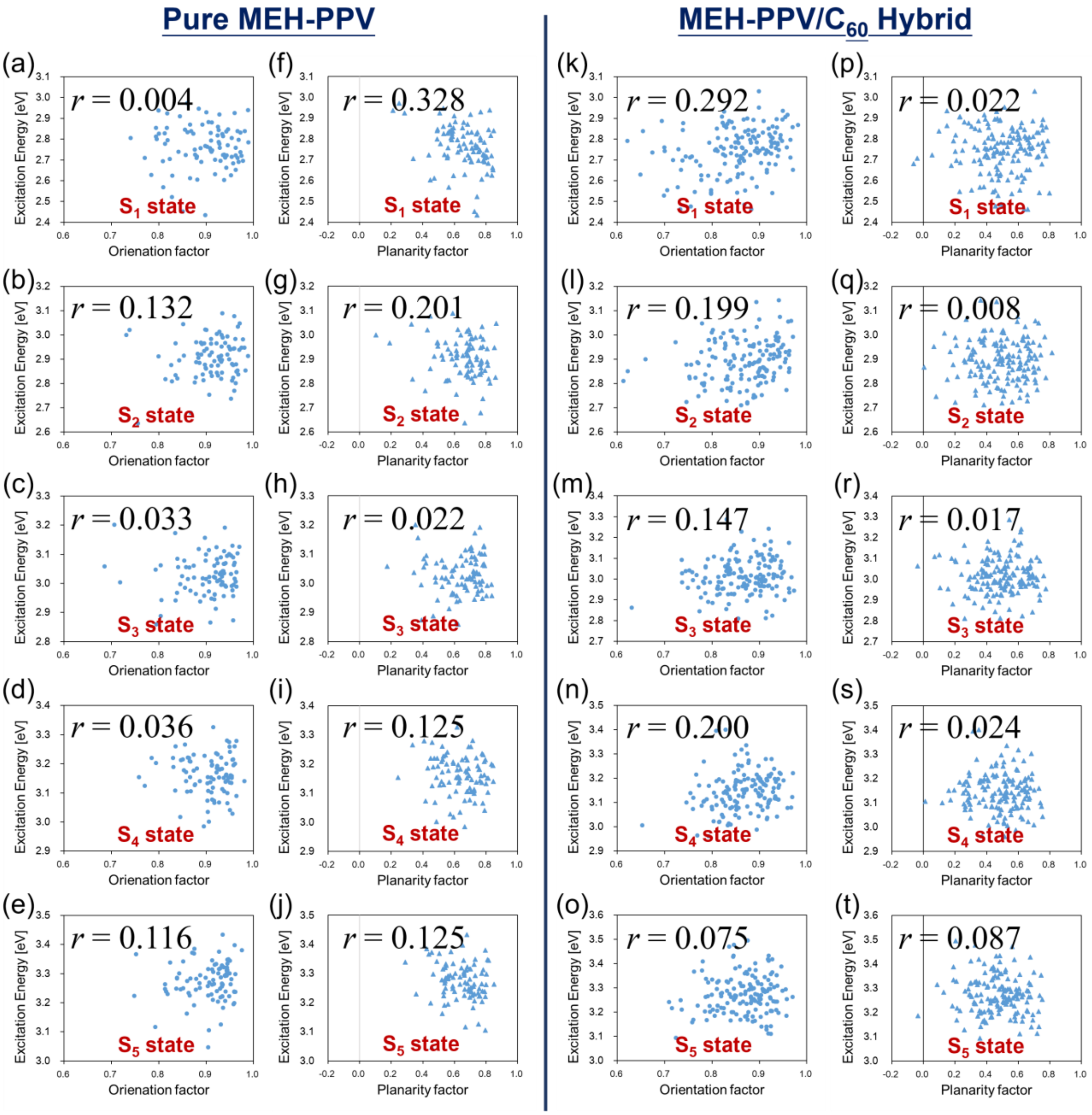

Fig. S8. Correlation analysis of the excitation energy with respect to two different conformational factors for the five lowest singlet excited states, for pure MEH-PPV (left panels) and MEH-PPV/C$_{60}$ hybrid (right panels) systems.

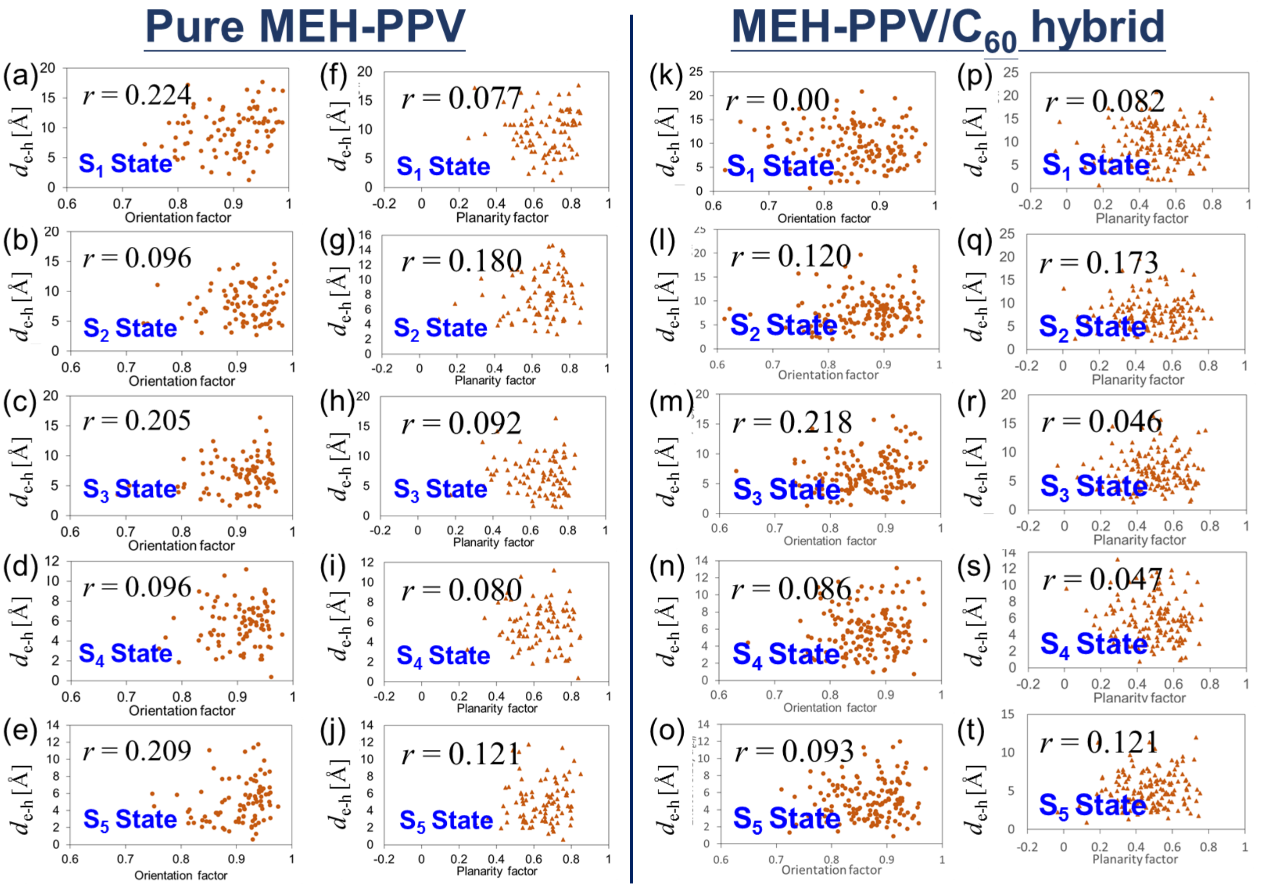

Fig. S9. Correlation analysis of the exciton size ($d_{\text{e-h}}$) with respect to two different conformational factors for the five lowest singlet excited states, for pure MEH-PPV (left panels) and MEH-PPV/C_{60} hybrid (right panels) systems, where $d_{\text{e-h}}$ was evaluated using an approximate method as described in ref 7 (ref 91 in the main text).

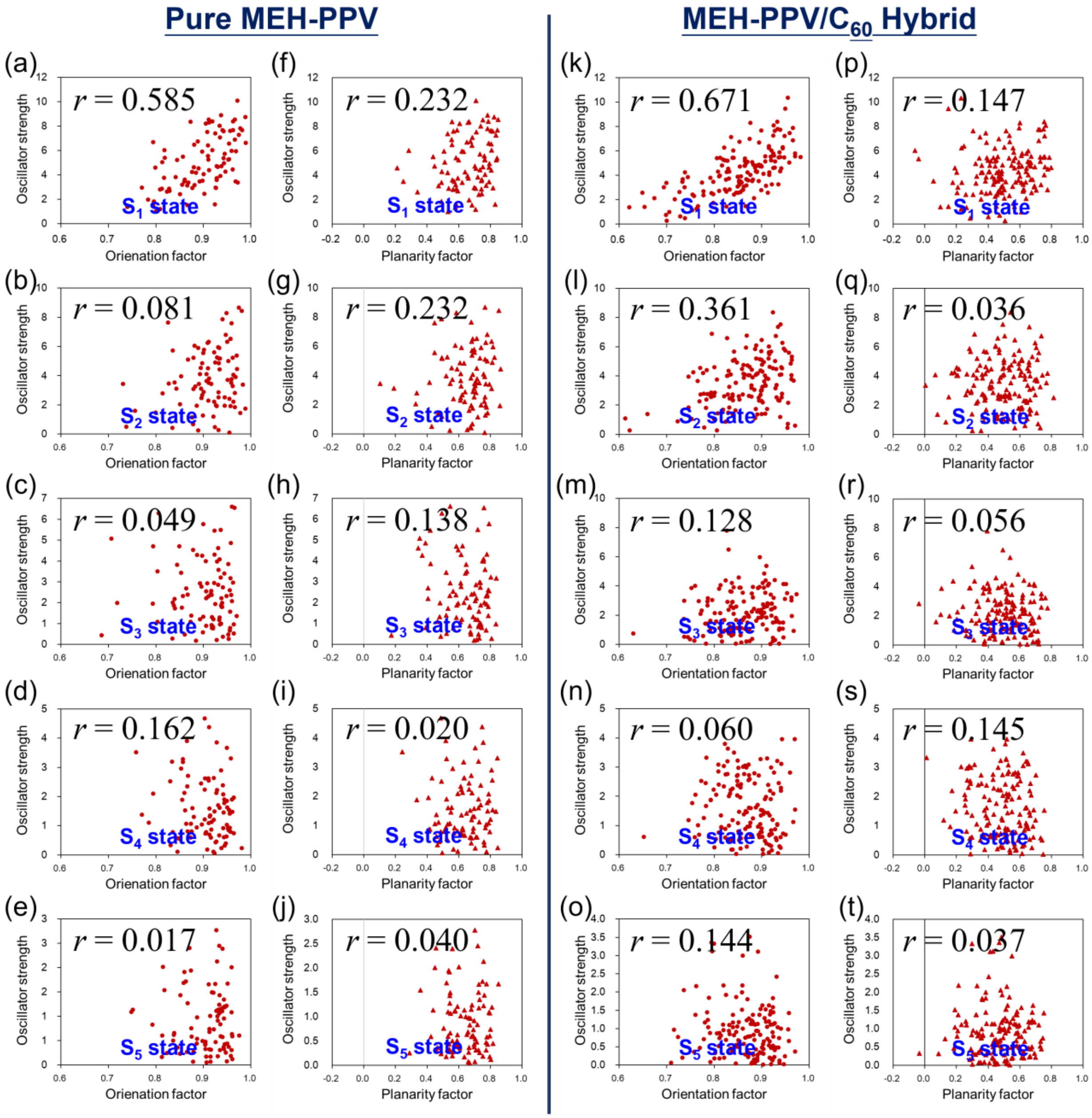

Fig. S10. Correlation analysis of the oscillator strength with respect to two different conformational factors for the five lowest singlet excited states, for pure MEH-PPV (left panels) and MEH-PPV/C$_{60}$ hybrid system (right panels).

References

1 K. H. DuBay, M. L. Hall, T. F. Hughes, C. Wu, D. R. Reichman and R. A. Friesner, *J. Chem. Theory Comput.*, 2012, **8**, 4556-4569.

2 W.-C. Ou-Yang, C.-S. Chang, H.-L. Chen, C.-S. Tsao, K.-Y. Peng, S.-A. Chen and C. C. Han, *Phys. Rev. E*, 2005, **72**, 031802.

3 A. N. Panda, F. Plasser, A. J. A. Aquino, I. Burghardt and H. Lischka, *J. Phys. Chem. A*, 2013, **117**, 2181-2189.

4 S. Tretiak, A. Saxena, R. L. Martin and A. R. Bishop, *Phys. Rev. Lett.*, 2002, **89**, 097402.

5 S. J. Martin, H. Mellor, D. D. C. Bradley and P. L. Burn, *Opt. Mater.*, 1998, **9**, 88-93.

6 I. Miller, J. Freund and R. A. Johnson, *Miller and Freund's Probability and Statistics for Engineers*, Pearson Education, Upper Saddle River, NJ, 2004.

7 H. Ma, T. Qin and A. Troisi, *J. Chem. Theory Comput.*, 2014, **10**, 1272-1282.